Mesoscopic-capacitor effect in $GaN/Al_xGa_{1-x}N$ quantum wells: Effects on the electronic states

A. Di Carlo, A. Reale, and P. Lugli
INFM, Department of Electronic Engineering, University of Rome ''Tor Vergata,'' Rome, Italy

G. Traetta, M. Lomascolo,* A. Passaseo, and R. Cingolani
INFM, Department of Innovation Engineering, University of Lecce, Via Arnesano, I-73100, Lecce, Italy

A. Bonfiglio
INFM, Electric and Electronic Engineering Department, University of Cagliari, Cagliari, Italy

M. Berti, E. Napolitani, M. Natali, S. K. Sinha, and A. V. Drigo
INFM, Department of Physics, University of Padova, Via Marzolo 8, I-35131 Padova, Italy

A. Vinattieri and M. Colocci
INFM, Department of Physics and LENS, Largo E. Fermi 2, I-50125 Firenze, Italy
(Received 1 December 2000; published 17 May 2001)

We show that wide GaN quantum wells behave like mesoscopic capacitors. The electron-hole pairs are separated by the spontaneous and piezoelectric polarization fields and accumulated in the well, resulting in a well-width dependent screening of the built-in field. The extent to which such screening is effective depends on the interplay between radiative and nonradiative recombination probabilities, which deplete the ground level of the quantum well, causing the recovery of the unscreened built-in field. The account of the mesoscopic capacitor effect provides a quantitative description of the optical spectra and of the time dynamics of a set of high quality quantum wells with well characterized structural parameters.

DOI: 10.1103/PhysRevB.63.235305 PACS number(s): 78.66.−w, 73.21.−b

I. INTRODUCTION

The recent developments in the field of GaN-based blue-UV optoelectronic devices[1] have stimulated several experimental and theoretical studies on $GaN/Al_xGa_{1-x}N$ multiple quantum wells (MQW's). Most of the attention has been paid to the existence of built-in electric fields in such heterostructures. The theory of Bernardini and Fiorentini[2–4] establishes that the internal electric field is originated by the difference in the spontaneous polarization between the barrier and the well, and by the piezoelectric polarization, due to the pseudomorphic growth of the well or of the barrier, depending on the buffer layer.

Several experiments have indeed shown that the ground level emission of thick $Al_xGa_{1-x}N/GaN$ quantum wells (QW's) falls below the energy gap of the bulk GaN.[5–12] Though this is a confirmation of the presence of an internal electric field, there is still a quantitative disagreement between the experimental ground-level energy deduced by the optical experiments and the calculated energy in the presence of the built-in electric fields. To circumvent this problem, the experimental data are usually fitted by using either the value of the electric field as a free parameter[7–12] or, in more refined self-consistent models,[5–6,13] by adjusting the actual carrier density in the well to screen the built-in field. In both cases, either the adjusted electric field (which is different from the real value) or the rather large injected carrier density (somewhat unphysical for a cw optical excitation) indicates that a quantitative understanding of the optical properties of GaN quantum wells is still somehow unresolved.

In this paper we present a different approach to the problem based on the idea that the GaN quantum wells behave like mesoscopic capacitors. We demonstrate that the charge density in the well is influenced by two main effects: (i) the separation of the wave functions, induced by the built-in field, which causes the increase of the radiative recombination time, and (ii) the loss of carriers from the ground level induced by both radiative and nonradiative recombination processes. The first effect, hereafter referred to as mesoscopic-capacitor effect, leads to the build-up of an electron-hole plasma in the well which screens the built-in field, resulting in a screening induced blue shift which partly compensates the red shift induced by the built-in field. This becomes more and more important in wide wells by virtue of the increased decay time (wave function separation), causing the charge accumulation at the interfaces.[13] The second effect, partly compensated by the charge accumulation, causes the recovery of the built-in field value expected for zero charge density. The proper account of these phenomena provides a new insight in the coupling of GaN/AlGaN structures with light, which has both fundamental and applied relevance.

II. EXPERIMENTAL STUDY

The samples were grown on (0001) *c*-plane Al_2O_3 substrates in a horizontal LP-MOCVD system (AIXTRON 200 AIX RE) equipped with a rotating substrate holder with TMGa, TMAl, and pure NH_3 as source materials. After the deposition of a low-temperature nucleation layer, a GaN buffer layer, 1-μm thick, was grown at 1150 °C followed by ten identical $GaN/Al_{0.15}Ga_{0.85}N$ wells of nominal width

TABLE I. Experimentally determined well width and Al content of the heterostructures investigated in this work. The experimental accuracy in the Al content is of the order of $\pm 1\%$.

Sample	QW1	QW2	QW3	QW4	QW5
Well width (nm)	1.6	2.4	3.2	6.3	9.5
Al content (% at.)	18.6	18	14.1	17.7	13.1

$2\ \text{nm} < L < 10\ \text{nm}$ and barrier width 15 nm.

The structural parameters of the samples were obtained by x-ray diffraction (XRD), Rutherford back scattering (RBS), and high resolution secondary-ion mass spectrometry (SIMS). The preliminary optimization of the GaN buffer layers resulted in a channeling yield $\chi_{\min}$ of about 1.5% in all samples (which is close to the theoretical value for an ideal sample). In addition, narrow full width of half maximum (FWHM) of the (002) peak, varying between 380 and 410 arc sec, was observed in the XRD measurements together with a clear step-flow surface morphology. The XRD measurements on the QW's gave the period of the heterostructures, whereas the RBS measurements allowed us to measure the average composition and total thickness, from which an independent value of the period was extracted in excellent agreement with the XRD measurements. The exact sample parameters are reported in Table I and were found to be close to the nominal values. The comparison between the XRD measurements of the lattice parameters of the GaN buffer layer and the MQW's layer reveals the pseudomorphic growth of the $Al_xGa_{1-x}N$ barriers on the GaN buffer.

More importantly, the compositional abruptness of the interfaces was verified by high resolution SIMS measurements, using a 1.6 keV O_2^+ ion primary beam at grazing incidence and detecting the secondary $^{27}A^+$ ions emitted from the samples as a function of depth. The results of Fig. 1 demonstrate the excellent sharpness of the interfaces with good periodicity throughout the entire superlattice, and resolution limited broadening (the slopes at the interfaces reduce by $1/e$ in 1.2 nm). This clearly indicates that Al interdiffusion in our samples is negligible, allowing us to discard important variations of the quantum well potential profile which would affect substantially the ground-level energy. Such a structural characterization was a fundamental step of this work since it allowed us to perform a quantitative analysis of the optical spectra without uncontrolled structural parameters (namely, well width and composition profile) to be used in the theoretical model. The photoluminescence (PL) measurements were performed either under cw excitation (325 nm line of a He-Cd laser) or under ps pulsed excitation (III-harmonic of a mode-locked Ti:sapphire). The time-resolved experiments were performed by using a frequency-doubled R6G dye-laser, synchronously pumped by the second harmonic of a mode-locked Nd:YAG laser. The samples were excited with 3 ps long pulses at an energy of 4 eV and an average power of a few mW. A cryostat was used to keep the samples at 10 K the PL was dispersed by a monochromator and detected by a cooled microchannel plate photomultiplier by means of a time-correlated single photon-counting apparatus with a time resolution of 50 ps.

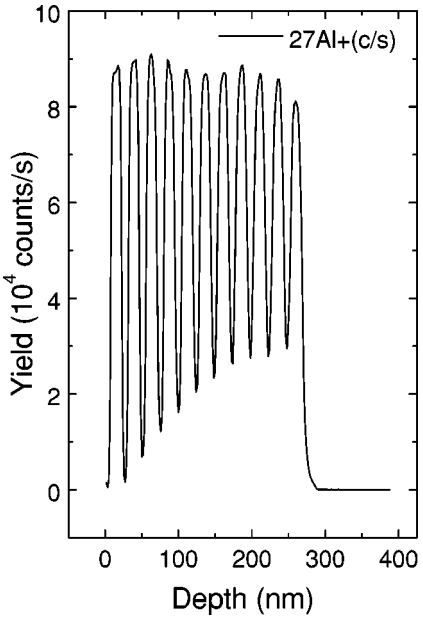

FIG. 1. SIMS Al depth profile of sample QW5.

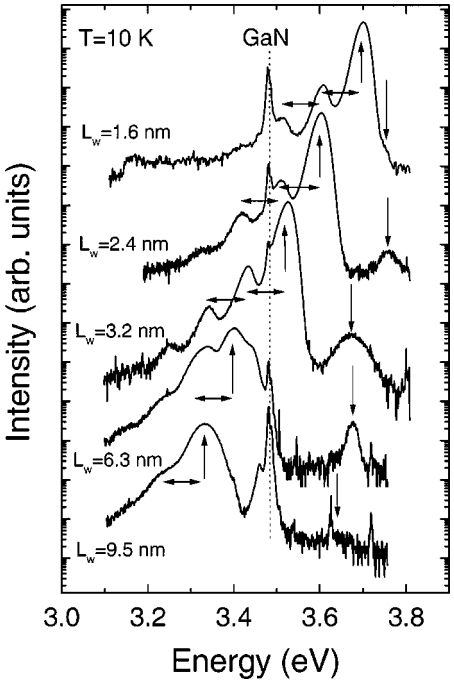

FIG. 2. Photoluminescence spectra of the samples measured at 10 K.

III. RESULTS

In Fig. 2 we show the low-temperature (10 K) PL spectra from 5 samples under cw excitation from a He-Cd laser (325 nm, about 5 mW power). The main characteristics of the spectra are the following:

(a) The overall red-shift of the emission bands with increasing the well width.

(b) The sharp peak at 3.48 eV due to the exciton of the

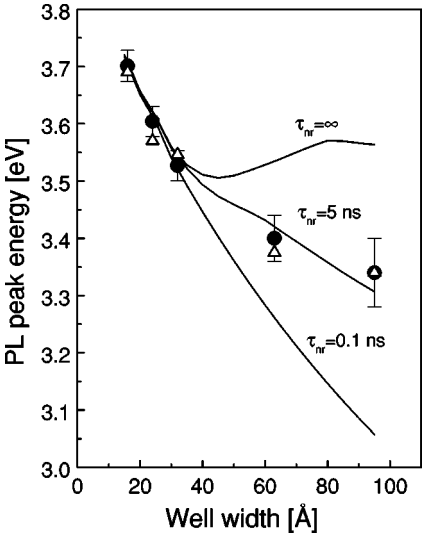

FIG. 3. Experimental (circles) and theoretical values (lines and triangles) of the emission energy of the samples. The lines show the theoretical calculation performed using an average Al barrier concentration of 15% and considering three different values of the nonradiative lifetime τ_{nr}: 0.1 ns, 5 ns and ∞. The curve with $\tau_{nr}=0.1$ ns is equivalent to the usual calculation accounting for the built-in field without mesoscopic capacitor effect. The triangles show the calculation obtained by using the values of Table I and a nonradiative recombination time of 5 ns.

GaN bulk layer in all the samples (dashed vertical line).

(c) The emission spectra falls below the bulk GaN energy for well widths larger than 3 nm (which is typical of the structures with internal electric fields).

(d) The strong decrease of the ground-level emission intensity (upward arrows) with increasing the well width, suggesting a reduction of the absorption induced by the separation of the electron and hole wave functions, and/or an important role of the nonradiative recombination channels.

(e) The slightly different emission energy from the Al-GaN barrier due to the differences in the Al content in the barriers (downward arrows).

(f) Several phonon replica separated from the zero phonon line by about 90 meV (horizontal markers).

The well-width dependence of the emission energy is calculated by using the envelope-function approximation, including the piezoelectric field and the spontaneous polarization,[2,13] and taking the actual Al-content and well width (see Table I). The details of the calculations can be found in Ref. 13. As shown in Fig. 3, the results predicted by the model when assuming a value of $\tau_{nr}=0.1$ ns which corresponds to an unscreened polarization field, describe quite well the ground-level energy of narrow wells, whereas they underestimate the values for wide wells. As mentioned above, such a disagreement cannot be ascribed to structural defects or indetermination in the structural parameters.

In order to get a deeper insight into the effective recombination channels, both radiative and nonradiative, in our quantum wells, we have performed time-resolved photoluminescence (TRPL) experiments. We show in Fig. 4 two representative TRPL curves taken at the peak of the emission

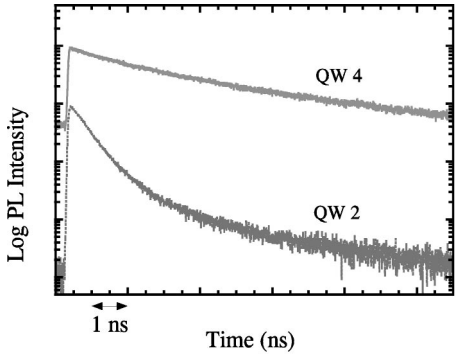

FIG. 4. Time-resolved photoluminescence curves at 10 K for samples 2 and 4. The PL was detected at the peak of the emission spectra for both samples. Normalization is arbitrary.

spectra of sample 2 and 4. The main features are (i) with increasing the well width, the temporal evolution of the photoluminescence intensity becomes slower; and (ii) the TRPL traces cannot be described, in general, by a single exponential decay. These results are in good agreement with those reported in literature[14] and confirm the picture of the increasing electron-hole wave function separation, with increasing the well width, induced by the quantum confined Stark effect[15] and consequent increase in the recombination lifetimes.

IV. THEORY AND COMPARISON WITH THE EXPERIMENT

In order to describe correctly the experimental data presented in the previous section it is necessary to develop a complete theoretical model that properly accounts for the process of generation and recombination of the electron-hole pairs, hereby including the effect of screening of the built-in field induced by the charging of the quantum well in the presence of wave function separation and increase of the electron-hole pair lifetime. We will assume a very simple model for the time evolution of the carrier density in the quantum well, that is

$$\frac{dn}{dt}=G-R_{sp}-R_{nr}, \tag{1}$$

where G is the generation rate, R_{sp} is the spontaneous (radiative) recombination rate, and R_{nr} is the nonradiative recombination rate.

Under steady-state conditions, and assuming a constant generation rate in all samples, Eq. (1) becomes

$$G=R_{sp}+R_{nr}, \tag{2}$$

which has to be solved for all samples by accounting for the dependence of R_{nr} and R_{sp} on the carrier density.

The spontaneous recombination rate R_{sp} is given by the proper integration of the absorption coefficient,[16]

$$R_{sp}=\int_{-\infty}^{+\infty}\frac{e^2\mu E_p\omega n_r}{\hbar^2c^3\pi^3\varepsilon_0 m_0}f_c(1-f_v)\sum_{i,f}I_{i,f}^2\theta(\omega-\omega_{if})d\omega, \tag{3}$$

TABLE II. Experimental emission energy and theoretical values of the emission energy, carrier density and spontaneous recombination rate for all the quantum wells considered in the study.

Sample	Experim. emission energy (eV)	Theoret. emission energy (eV)	Charge density n (cm^{-2})	Spontaneous recombination rate ($cm^{-2}\,s^{-1}$)
QW1	3.701 ± 0.027	3.690	3.21×10^{11}	5.03×10^{20}
QW2	3.604 ± 0.026	3.570	5.90×10^{11}	4.65×10^{20}
QW3	3.527 ± 0.026	3.546	7.61×10^{11}	4.36×10^{20}
QW4	3.40 ± 0.04	3.375	2.77×10^{12}	9.1×10^{18}
QW5	3.34 ± 0.06	3.340	2.82×10^{12}	4.26×10^{16}

where all the symbols have their usual meaning,[16] n_r is the refractive index, f_c, f_v are the Fermi distributions, θ is the Heavyside function, $I_{i,f}$ is the wave function overlap, and ω_{if} is the energy transition from the initial level i in conduction band to the final level f in valence band. In Eq. (3) both quasi-Fermi levels, overlap matrix elements, and transition energy are all charge density dependent. Overlap and transition energy are related to the density through the coupling between the Poisson and Schöedinger equations. Equation (3) represents the microscopic expression of the bimolecular recombination term which is widely used in rate equation models describing carrier dynamics in QW's.

The nonradiative recombination rate accounts for all the nonradiative recombination channels, such as defects assisted and surface recombination,[15] for the sake of simplicity, we will assume a very simple expression for R_{nr}, that is

$$R_{nr} = \frac{n}{\tau_{nr}} \tag{4}$$

with the time constant τ_{nr} equal for all the wells.

A double iteration is performed in order to determine the actual carrier density and energy levels. Assuming an initial photogenerated carrier concentration, the energy of quantized levels needed for the evaluation of the spontaneous recombination rate is obtained by self-consistently solving Schröedinger and Poisson equations. Equation (2) is then solved for n, and this value is put again into the Schröedinger-Poisson solver. The two-step procedure is repeated until convergence is achieved. In the calculations the value of the nonradiative carrier lifetime τ_{nr} has been assumed to be of the order of 5 ns, as suggested by the TRPL curves of wider well, where the radiative recombination rates are an order of magnitude longer due to the decrease of the wave function overlap (see also Table II). Therefore, the nonradiative decay is not a fitting parameter in the comparison between theory and experiment. Such a nonradiative lifetime is obviously typical of our samples. However, even though it can change depending on the growth technique, doping, and, sample and substrate quality, similar lifetimes have been obtained by other groups.[14,17]

As shown in Fig. 3, the experimental data (dots) are well reproduced by the theory (solid lines) with $\tau_{nr} = 5$ ns. For the sake of comparison we also plot the limiting cases of a negligible nonradiative recombination rate (i.e., $\tau_{nr} = \infty$) and of a dominant nonradiative recombination ($\tau_{nr} = 0.1$ ns). In the absence of nonradiative recombinations, the mesoscopic-capacitor effect is dominant, especially for wide wells. On the contrary, a strong nonradiative rate depletes the ground level, preventing charge accumulation and thus leaving the field unscreened. Indeed, the result coincides perfectly with that obtained in the absence of free carriers. The flattening of the PL peak energy observed in the experiment at increasing well width is therefore due to the competition between radiative and nonradiative recombination processes. For the larger wells, the built-in field is effectively screened due to the mesoscopic-capacitor effect, that is to the charge accumulation favored by the long radiative lifetime (which is, in turn, a consequence of the spatial separation of the electron and hole wave functions). On the contrary, nonradiative recombinations tend to deplete the ground level energy, thus reducing the effect of screening and red-shifting the PL spectra.

Table II summarizes our results, showing the transition energy, carrier density and spontaneous recombination rate R_{sp} for all the quantum wells considered in the study. The spontaneous recombination rate R_{sp} for the 1.6 nm quantum well is indeed found to be several orders of magnitude larger than that of the 9.5 nm well. Consistently, the carrier density is largest in the 9.5 nm well.

These results have important consequences on the optical properties of GaN quantum wells, not only concerning the shift of the ground-level energy, but also the strength of the excitonic resonances. In fact, these results show that a cw pumping in the mW range is enough to induce a plasma density ranging between about 3×10^{11} and 3×10^{12} depending on the well width. This causes a strong reduction of the exciton binding energy and of the absorption coefficient, as predicted in Ref. 18, thus modifying the electric-field induced and the many-body nonlinearities of GaN OW's.

V. CONCLUSIONS

In conclusion we have demonstrated that in $GaN/Al_xGa_{1-x}N$ quantum wells the separation of the wave function due to the built-in electric field induces long radiative lifetimes which in turn lead to a charge accumulation in the wells. This capacitor effect is only partially compensated by the nonradiative recombination channels and it becomes increasingly important in wider wells, where the separation of the wave functions is larger. The results of our theoretical model, taking into account self-consistently the screening of the electric field and recombination of the electron-hole pairs, are in good agreement with the experimental ground-level emission energy of these structures. Moreover the results shown that any estimation of polarization field by cw experiments should consider the mesoscopic-capacitor effect.

ACKNOWLEDGMENTS

The expert technical help of D. Cannoletta, A. Melcarne, and I. Tarantini is gratefully acknowledged. This work has been partially supported by MURST, INFM, and UE Net-

work ''Ultrafast Quantum Optoelectronics'' and ''CLERMONT.''

*Permanent address: Istituto per lo studio dei nuovi materiali per l'elettronica IME-CNR, Campus Universitario, Via per Arnesano, 73100, Lecce (Italy).

[1] For a review see, S. Nakamura and G. Fasol, *The Blue Laser Diode* (Springer-Verlag, Berlin, 1997).
[2] F. Bernardini, V. Fiorentini, and D. Vanderbilt, Phys. Rev. B **56**, R10 024 (1997).
[3] F. Bernardini, V. Fiorentini, and D. Vanderbilt, Phys. Rev. Lett. **79**, 3958 (1997).
[4] F. Bernardini and V. Fiorentini, Phys. Rev. B **57**, R9472 (1998).
[5] R. Cingolani *et al.*, Phys. Rev. B **61**, 2711 (1999).
[6] A. Bonfiglio *et al.*, J. Appl. Phys. **87**, 2289 (2000).
[7] M. Leroux *et al.*, Phys. Rev. B **58**, R13 371 (1998).
[8] M. Leroux *et al.*, Phys. Rev. B **60**, 1496 (1999).
[9] T. Takeuchi *et al.*, Appl. Phys. Lett. **73**, 1691 (1998).
[10] T. Takeuchi *et al.*, Jpn. J. Appl. Phys., Part 2 **36**, L382 (1997).
[11] S. H. Park and S. L. Chuang, Appl. Phys. Lett. **72**, 3103 (1998).
[12] J. S. Im *et al.*, Phys. Rev. B **57**, R9435 (1998).
[13] F. Della Sala *et al.*, Appl. Phys. Lett. **74**, 2002 (1999); A. Di Carlo *et al.*, *ibid.* **76**, 3950 (2000).
[14] J. C. Harris, T. Someta, K. Hoshino, S. Kako, and Y. Arakawa, Phys. Status Solidi A **180**, 339 (2000); Appl. Phys. Lett. **77**, 1005 (2000).
[15] P. Bhattacharya, *Semiconductor Optoelectronic Devices* (Prentice-Hall Inc., Upper Saddle River, NJ, 1994).
[16] K. Ebeling, *Integrated Opto-electronics* (Springer-Verlag, Berlin, 1992).
[17] K. C. Zeng *et al.*, Appl. Phys. Lett. **71**, 1368 (1997).
[18] G. Traetta *et al.*, Appl. Phys. Lett. **76**, 1042 (2000).